

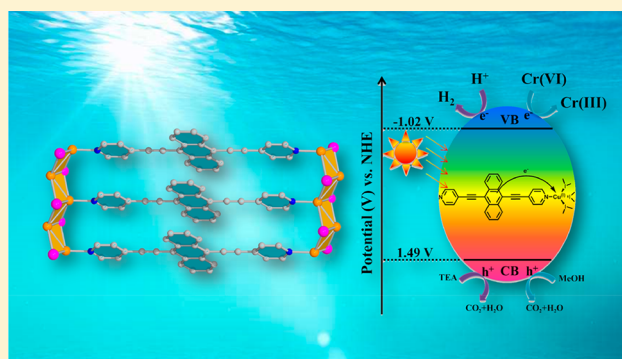
Stable Layered Semiconductive Cu(I)–Organic Framework for Efficient Visible-Light-Driven Cr(VI) Reduction and H₂ Evolution

Di-Ming Chen, Chun-Xiao Sun, Chun-Sen Liu,*^{ORCID} and Miao Du*^{ORCID}

College of Material and Chemical Engineering, Zhengzhou University of Light Industry, Zhengzhou 450002, P. R. China

Supporting Information

ABSTRACT: Metal–organic frameworks (MOFs) have gained tremendous attention in the fields of environmental restoration and sustainable energy for their potential use as photocatalyst. Herein, a new two-dimensional (2D) Cu(I)-based MOF material showing a narrow forbidden-band of 2.13 eV was successfully constructed using a visible-light-harvesting anthracene-based bipyridine ligand. The as-prepared MOF demonstrates high chemical stability and could be stable in the pH range 2–13, which is favorable for its potential application in photocatalysis. Photocatalytic experiments demonstrate that this Cu(I)-MOF exhibits high reactivity for reduction of Cr(VI) in water, with 95% Cr(VI) converting to Cr(III) in 10 min by using MeOH as scavenger under visible-light illumination. Furthermore, this MOF could behave as a highly active photocatalyst for H₂ evolution without additional photosensitizers and cocatalyst. Remarkably, the as-prepared MOF shows enhanced photocatalytic Cr(VI) reduction and H₂ evolution performances compared with the pristine light-harvesting ligand under the same conditions. In connection to these, the photocatalytic reaction mechanism has also been probed.



INTRODUCTION

With the fast evolution of industry, increasing concerns about the energy crisis and environmental pollution have been faced by people all over the world. With the purpose of solving the increasing demand for sustainable energy and the accompanied environmental pollutions of modern industry, great endeavors have been dedicated to the developing new technology using renewable solar light through photocatalysis.^{1–6} As a common heavy metal pollutant in effluent generated by industrial production such as leather-making, electroplating, and chemical metallurgy, Cr(VI) is notorious for its nonbiodegradation and high toxicity.^{7–9} The transformation of Cr(VI) to Cr(III) through reductive reactions is considered to be an effective approach to eliminate Cr(VI) from wastewater because Cr(III) is less soluble in water though formation of the (hydr)oxides and shows less toxicity than Cr(VI).¹⁰ In comparison with chemical reduction and electroreduction, the visible-light-driven transformation of Cr(VI) to Cr(III) using photocatalysts has more prospects, because it does not generate additional harmful chemicals and is low-cost. A series of semiconductors such as CdS, SnS₂, and Ag₂S has been used as photocatalysts for reduction of Cr(VI).^{11–13} However, the use of sulfide reagents in the photocatalytic process sometimes is subjected to photocorrosion and may lead to the generation of secondary pollutants. In this case, the search for stable photocatalysts for effective Cr(VI) reduction is of high importance. On the other hand, H₂ is considered as a promising chemical fuel for future application because of its

high energy density and renewability. It has been reported that the photogenerated H₂ evaluation is one of the most promising approaches for the production of H₂ from water.^{14–17}

Composed of metal nodes and organic linkers, metal–organic frameworks (MOFs) have emerged as a promising kind of crystalline material due to their adjustable compositions and designable topological networks.¹⁸ The rich selection of light-harvesting building blocks makes this kind of material an ideal platform for application in the artificial photosynthetic systems.¹⁹ To date, several MOF-based photocatalysts have been studied either in aqueous Cr(VI) reduction or H₂ evolution such as NH₂-MIL-88, NH₂-MIL-100 (Fe), NH₂-MIL-125(Ti), and NH₂-UiO-66 (Fe).^{20–24} For example, Wang and co-workers have demonstrated the employment of the NH₂-MIL-125(Ti) as photocatalyst for effective reduction of Cr(VI); Gascon et al. have prepared a noble-metal-free Co@NH₂-MIL-125(Ti) composite as recyclable catalyst for water splitting under visible-light irradiation. However, to our knowledge, no dual-functional MOF-based photocatalyst for both Cr(VI) reduction and H₂ evolution has been reported, especially without the presence of cocatalyst and photosensitizer in the reaction systems.

In this work, a new 2D Cu(I)-based MOF material showing a narrow forbidden-band of 2.13 eV was successfully constructed by employing a visible-light-harvesting anthra-

Received: April 25, 2018

cene-based bipyridine ligand. The as-prepared MOF demonstrates high chemical stability which could be stable in the pH range 2–13. Photocatalytic studies demonstrate that this Cu(I)-based MOF exhibits high reactivity for reduction of Cr(VI) in water, with 95% Cr(VI) converting to Cr(III) in 10 min by using MeOH as scavenger (pH = 3.09) under visible-light irradiation. Furthermore, this MOF could behave as a highly active photocatalyst for H₂ evolution without adding any photosensitizers and cocatalyst. In connection to these, the possible photocatalytic mechanism has also been discussed.

EXPERIMENTAL SECTION

Chemicals and Testing Methods. All the reagents were bought commercially and used as received. The Vario EL III Elemental analyzer was used to get the elemental analysis results of the C, H, and N content. The Rigaku model Ultima IV diffractometer with Cu K α radiation was employed to collect the PXRD curves at room temperature. The TGA curve in the range 25–800 °C was obtained on the Netzsch STA-409CD thermal analyzer. The Mott–Schottky plots were measured on a three-electrode electrochemical workstation (Solartron ModuLab XM Instruments). The luminescent spectra were obtained from the fluorescence spectrophotometer (Cary Eclipse Agilent). X-ray photoelectron spectroscopy (XPS) analysis was conducted on the AXIS HIS 165 spectrometer (Kratos Analytical, Manchester, UK).

Synthesis of [Cu₂I₂(BPEA)](DMF)₄ (1). Into a Teflon vessel (25 mL) was added a mixture of BPEA (0.02 mmol, 7.6 mg), CuI (0.04 mmol, 7.6 mg), EtOH (2 mL), HCOOH (0.1 mL), DMF (3 mL), and CH₃CN (5 mL). The vessel was heated at 423 K for 48 h. After slowly cooling the reaction system to ambient temperature, yellow crystals for **1** were harvested, washed with DMF (2 × 3 mL), and dried at room temperature. Yield: 32% (on the basis of the BPEA ligand used). Anal. Found (Calcd) for C₄₀H₄₄Cu₂I₂N₆O₄: H, 4.56 (4.21); C, 45.62 (45.59); N, 7.49% (7.98%).

X-ray Crystallography. The X-ray single-crystal data were measured on the Oxford SuperNova diffractometer using Cu K α radiation. The initial structure model was derived from the SHELXT program and then refined using the SHELXL program based on the least-squares technique.²⁵ All non-H atoms were treated anisotropically, and all hydrogen atoms are generated geometrically. The lattice DMF guests are highly disordered and difficult to locate in the refinements, so their electronic contributions are eliminated by the SQUEEZE manipulation in PLATON.²⁶ Table 1 shows the further details of structural refinement parameters of **1**.

Table 1. Crystalline Data and Refinement Parameters for **1**

formula	C ₁₄ H ₈ CuIN
fw	380.65
temp (K)	293(2)
cryst syst	monoclinic
space group	I ₂ /a
a (Å)	18.9903(7)
b (Å)	4.18100(10)
c (Å)	30.8429(12)
β (deg)	101.511(4)
V (Å ³)	2399.62(14)
Z	8
D _c (g cm ⁻³)	2.107
μ (mm ⁻¹)	22.539
R _{int}	0.0418
reflns collected/unique	2123
GOF on F ²	1.064
R ₁ , wR ₂ [I > 2 σ (I)]	0.0378, 0.1037
R ₁ , wR ₂ (all data)	0.0394, 0.1060
largest peak/hole (e Å ⁻³)	1.07/−1.08

Photocatalytic Experiments. The reduction of Cr(VI) was conducted in a 100 mL quartz reactor at ambient temperature. Into a quartz reactor was added a mixture of 40 mL of K₂Cr₂O₇ aqueous solution (10 ppm) and 15 mg of **1**. The pH values of the solution were modulated using 0.2 M NaOH and 0.2 M H₂SO₄. The mixture was stirred, and then MeOH was introduced. After being mixed for 80 min to achieve the desorption–adsorption balance in the dark, the quartz reactor was exposed to light illumination (Xe lamp) at room temperature. During each interval, about 1.5 mL of solution was taken from the quartz reactor, and the insoluble solid samples of **1** were separated by centrifugation. The diphenylcarbazide method (DPC) was used to get the absorbance of Cr(VI) in the solution.

Photocatalytic water splitting experiments were performed in a 25 mL quartz reaction flask. A 2 mg portion of **1** was added into a mixture of ethanol, deionized water, and triethylamine. The pH value of this suspension was modulated using HCl or NaOH and monitored with a pH meter. The flask was sealed with a septum, and the suspension was degassed by bubbling argon for 5 min. A 500 W Xe lamp was used to irradiate the suspension. The GC 7890T instrument was used to characterize the photoproduct of H₂, and the external standard method was used to determine the amount of H₂.

RESULTS AND DISCUSSION

Characterization of 1. Solvothermal reaction of CuI and BPEA ligand in a mixed solvent of DMF/EtOH/CH₃CN/HCOOH generates the yellow crystalline products of **1** with the formula [Cu₂I₂(BPEA)](DMF)₄. An X-ray structural analysis demonstrates that complex **1** locates in the monoclinic I₂/a space group with one I[−] ion, one Cu(I) ion, and half a BPEA ligand in the building unit. The distorted tetrahedral geometry of the four-coordinated Cu(I) ion is shaped by three I[−] ions and one pyridyl N donor from the BPEA ligand (Figure 1a). The adjacent Cu(I) ions are connected with each other via the μ_3 -bridge I[−] ions to shape a 1D ladder-like building unit along the *b* axis, which is further extended into a 2D layered structure by the BPEA ligand along the *a* axis (Figure 1b). The 2D layers are further stacked along the *c* axis to afford a 3D supramolecular structure (Figure 1c,d). There is a weight loss of 37.1% from 25 to 150 °C as revealed by the TGA curve, which might be ascribed to the escape of four lattice DMF molecules (Figure S1). The PXRD measurements were conducted to validate the phase purity of **1**, and they show a good match between the measured diffraction peaks and calculated ones from the crystal data, confirming the high phase purity of **1**.

Considering that the following photocatalysis studies were performed in water, the aqueous stability of **1** was checked correspondingly. The PXRD measurements show that complex **1** not only could be stable in aqueous solutions with pH values ranging from 2 to 13 but also could keep its framework integrity in boiling water for 1 day, showing its high water stability (Figure 2a and Figure S2). The optical absorbance of **1** was investigated by diffuse reflectance UV–vis analysis, and the corresponding result is depicted in Figure 2b. MOF **1** demonstrates significant visible-light absorption ability, and the absorption edge was found to be around 610 nm, which indicates its potential use as visible-light photocatalysis.²⁷ On the basis of the equation of $ah\nu = (h\nu - E_g)^{1/2}$, the calculated band gap value of **1** is 2.13 eV, implying that **1** could show a response to visible light (Figure 2c). In comparison, the BPEA ligand shows visible-light absorption with the edge at about 570 nm, which is an obvious blue-shift compared to that of **1**, indicating a broadening band gap (2.3 eV estimated from the UV–vis spectrum, Figure S3). The above results also illuminate that the HOMO–LUMO energy gap is reduced

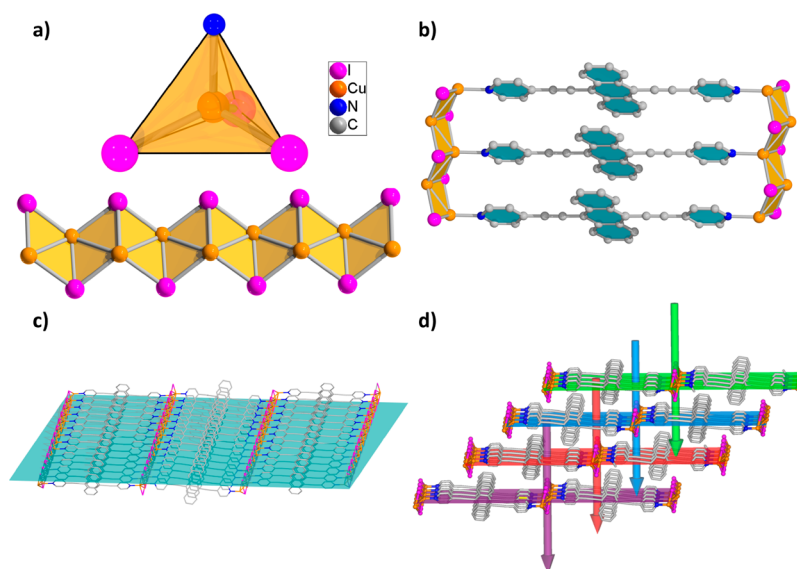


Figure 1. Views for (a) coordination surrounding the Cu(I) ion of **1**, (b) the connection of the adjacent CuI chains via the BPEA ligand, (c) the 2D layered network of **1**, and (d) the stacking of the 2D layers along the *c* axis.

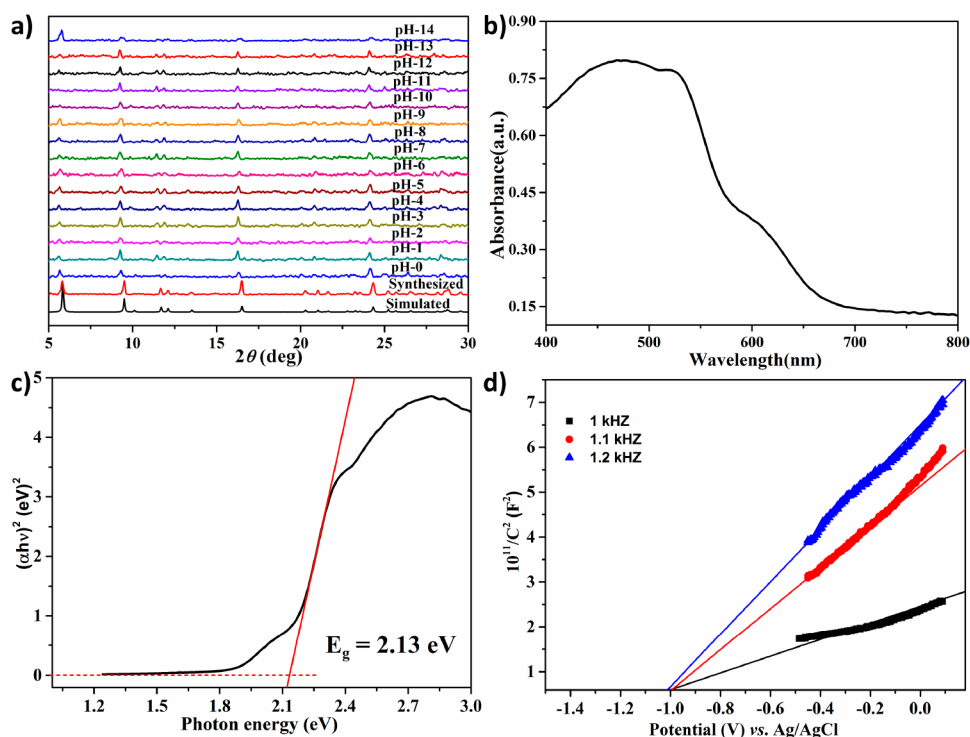


Figure 2. (a) pH-dependent PXRD patterns for **1**, (b) UV-vis spectrum of **1**, (c) plot of $(ah\nu)^2$ versus photon energy ($h\nu$) of **1**, and (d) Mott-Schottky plots of **1**.

though incorporation of the organic ligand BPEA into the framework of **1**, which makes the photoinduced electron-transfer (PET) process favorable.^{28,29} In order to evaluate the semiconductor property of **1**, Mott-Schottky plots were measured in 0.2 M Na₂SO₄ aqueous solution with the pH value of 6.8. Figure 2d displays that the flat-band potential of **1** derived from Mott-Schottky plots is -1.02 V versus the Ag/AgCl electrode, corresponding to a redox potential of the conduction band (CB) of -0.82 V versus normal hydrogen electrode (NHE) according to the Nernst equation, and this is more negative than the Cr(VI)/Cr(III) potential (0.51 V and

pH = 6.8).³⁰ The above results indicate that **1** has the potential for reduction of Cr(VI) to Cr(III). On the basis of the forbidden-band calculation discussed above, the valence band (VB) of **1** is 1.49 V vs NHE.

Photocatalytic Reduction of Cr(VI). The photocatalytic performance toward Cr(VI) reduction over **1** has been studied under visible-light conditions. Before the photocatalytic reduction, the K₂Cr₂O₇ solution was stirred in the dark for ca. 80 min to realize the desorption-adsorption balance, and the amount of Cr(VI) was monitored via the UV-vis adsorption spectra. To explain the photocatalytic character of

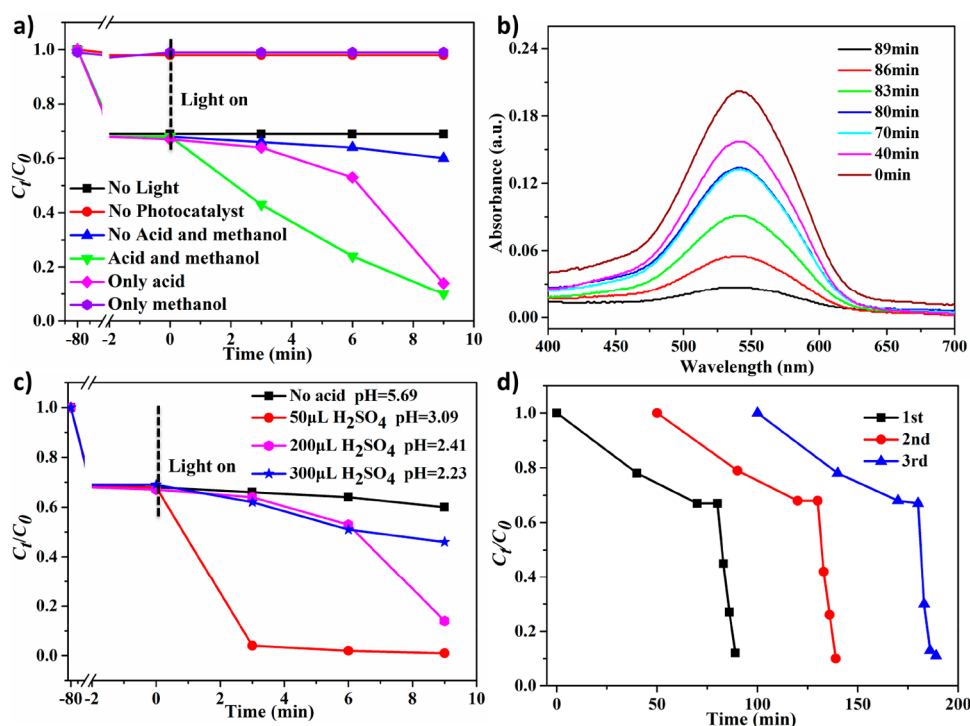


Figure 3. (a) Cr(VI) reduction reactions with different systems, (b) time-dependent adsorption spectra for DPC–Cr(VI) complex solutions, (c) pH-dependent photocatalytic Cr(VI) reduction over **1**, and (d) three runs of Cr(VI) reduction over **1** at pH 3.09.

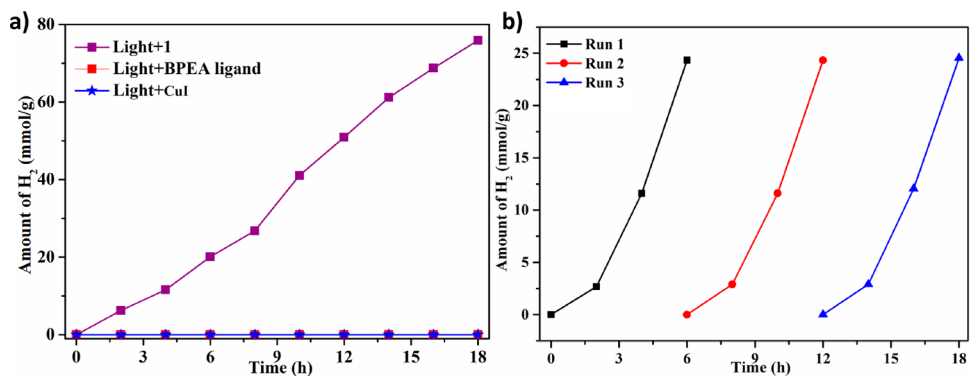


Figure 4. (a) Comparison study of photocatalytic H₂ evolution over **1**, BPEA ligand, and CuI. (b) Three cycles of photocatalytic H₂ evolution over **1**.

the Cr(VI) reduction, control tests were first conducted. As displayed in Figure 3a, it could be observed that the reduction of Cr(VI) hardly reacts without the presence of photocatalyst or light. In contrast, the amount of Cr(VI) is obviously decreased with the presence of hole scavenger and photocatalyst under visible-light illumination. The reduction ratio of Cr(VI) is 95% after visible illumination for 9 min, which is more efficient than those shown by NNU-36, NH₂-MIL-125(Ti), and UiO-66(NH₂) under similar conditions.^{20,27,31} The above results indicate that the Cr(VI) reduction reaction is a light-dependent process in which the hole scavenger and photocatalyst play vital roles. It has been reported that the pH value of the solution could greatly influence the reduction rate of aqueous Cr(VI) over photocatalyst, and in this case, controlled experiments have been conducted under different pH conditions.^{32–34} Figure 3b shows the time-dependent photocatalytic Cr(VI) reduction over **1** at different pH values adjusted by 0.2 M H₂SO₄. It could be found that the best pH

value is 3.09 in the controlled experiments. The observed Cr(VI) reduction performance of **1** was further compared with that of the BPEA ligand at the optimized condition. The results of the time-dependent photocatalytic Cr(VI) reduction reactions over the two systems are shown in Figure 3c. It is obvious that the Cu(I)-MOF possesses much higher photocatalytic Cr(VI) reduction activity than the BPEA ligand.

From the economic point of view, a good photocatalyst should have considerable stability and recycling. The durability of the photocatalytic activity of **1** in the Cr(VI) reduction process under visible-light illumination has been checked by the recycling experiments. The used photocatalyst was separated by filtration, washed with water, and used in the next cycle of experiment. As shown in Figure 3d, the photocatalytic activity of **1** shows no obvious decrease after three cycles of experiments, suggesting the high stability of **1** in the Cr(VI) reduction process. Furthermore, the PXRD patterns of **1** after three cycles of experiments reveal that the

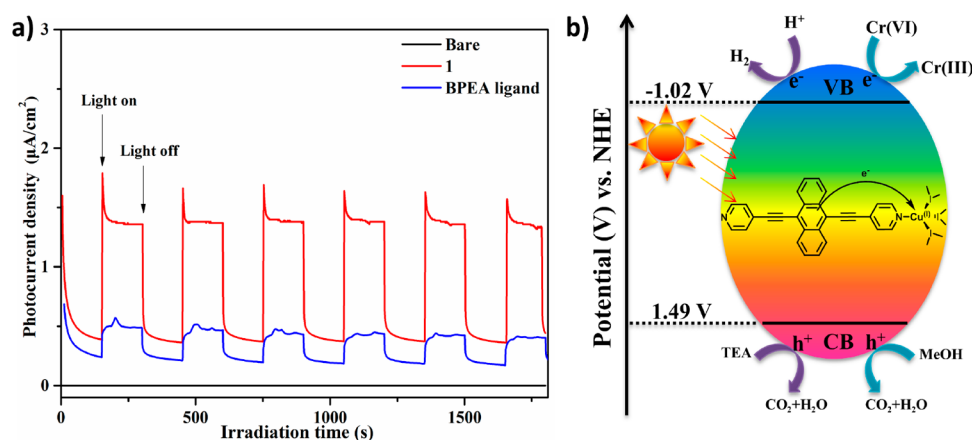


Figure 5. (a) Photocurrent response for the bare electrode, BPEA ligand, and **1** in 0.1 M KCl (aq). (b) Possible mechanism of Cr(VI) reduction and H₂ evolution over **1** exposed to visible-light irradiation.

framework keeps its integrality (Figure S5). The ICP analysis results demonstrate that there are no Cu(I) ions leaching from **1** during the reaction. In addition, the XPS results of the samples reveal that the valence state of Cu ion remains unchanged in the reduction process, and the weak peak located at 576.2 eV could be assigned to the Cr 2p_{3/2}, which is typically attributed to Cr³⁺, illuminating the reduction of Cr(VI) which occurs on the surface of **1** (Figures S6 and S7).³⁵ These results illuminate that both reusability and stability could be observed for **1** in this photocatalytic reaction.

Photocatalytic H₂ Evolution. The photocatalytic H₂ evolution activities of **1** were studied in the presence of triethanamine (TEA) as the hole scavenger. The reaction system is deoxygenated and exposed to visible-light illumination. The photocatalytic H₂ evolution amount is negligible in the presence of the ligand or CuI, demonstrating that neither the BPEA ligand nor the CuI could act as an efficient photocatalyst (Figure 4a). After the introduction of **1**, the H₂ evolution activity of the system is significantly enhanced. The amount of H₂ generated from the system increases with time and reaches about 75.89 mmol/g within 18 h irradiation. According to the literature, the pH value of the reaction system plays a vital effect on photocatalytic performances.^{36–38} In this case, 5 h of H₂ evolution over the as-prepared **1** at pH from 10 to 12.5 (adjusted by HCl and NaOH) was studied, and the results are shown in Figure S8, which indicates that the increase of pH value from 10.0 to 12.0 could boost the H₂ evolution amount, although a further increase in pH (greater than 12.0) results in a decrease of the H₂ evolution rate. The above experimental results indicate that the mild basic conditions might be propitious to the H₂ evolution reaction of **1**, and the optimized pH value is 12.0. To probe the framework stability of **1** in the photocatalytic process, the recycling experiments were carried out, and the results are shown in Figure 4b. The result reveals that the photocatalytic activity of **1** shows no obvious decrease after three recycles of experiments. Furthermore, the PXRD measurements also confirm the framework integrity of **1** after three recycles of experiments (Figure S9).

Photocatalytic Mechanism. To probe the plausible mechanism for **1** mediated photocatalysis, transient photocurrent responses have been carried out to assess the separation efficiency of photoinduced electron–hole pairs as well as to understand the interface charge transport behavior

(Figure 5a). When the light is turned on, **1** presents an obviously enhanced photocurrent intensity compared with that of the BPEA ligand. The average photocurrent intensity of **1** is about 4 times higher than that of the BPEA ligand. The higher photocurrent response of **1** might be explained by the long lifetime of the photogenerated hole–electron pairs in the 2D layered framework. Therefore, the photocurrent results demonstrate that the electron mobility of the BPEA ligand is greatly improved by forming MOF, resulting in the decreased recombination of photoinduced e[−]/h⁺, giving rise to the enhanced photocatalytic activity. According to the literature, the Cu(I)-based MOFs, containing Cu(I)–I chains as the building unit, have been demonstrated to have semiconductor properties.³⁹ To study the electron transfer in **1**, its (photoluminescence) PL spectra were collected at room temperature. As displayed in Figure S10, the PL spectrum of the BPEA ligand revealed a peak at 565 nm upon excitation at 300 nm, and this peak can be assigned to the intraligand emission. However, no PL signal could be observed for **1** around 565 nm with a new peak emerging around 490 nm, which indicates there is the ligand-to-metal charge-transfer.⁴⁰ According to the above analysis, the possible mechanism for the Cr(VI) reduction and evolution of H₂ over **1** has been proposed. In these processes, the BPEA ligands could behave as light-absorbing antennae, and the excited electrons from the ligand are able to transfer to the Cu(I) center. Upon light illumination, the excited electron on the CB of BPEA ligands jumps to the VB in the Cu(I) center, and then transfers to the Cr(VI) ion adsorbed on the MOF surface or H⁺ ion to form the Cr(III) ion or H₂, while the hole scavengers adsorbed on the MOF surface are oxidized by the photogenerated holes to form CO₂ and H₂O (Figure 5b).

CONCLUSION

In summary, a visible-light active layered Cu(I)-MOF material showing a narrow forbidden-band of 2.13 eV was successfully prepared by using a visible-light-harvesting anthracene-based bipyridine ligand. The as-prepared material not only exhibited superior chemical stability which could keep its framework integrity in the wide pH range 2–13 but also demonstrates excellent photocatalytic activity for reduction of Cr(VI) and H₂ evaluation in water. Furthermore, such photocatalytic processes do not need the aid of additional photosensitizers and cocatalyst, which is quite rare among MOF-based

photocatalysis. In addition, the obtained MOF shows better photocatalytic performance than that of the pristine organic ligand, indicating that the introduction of visible-light-harvesting ligands into MOFs is a promising approach for fabricating MOF-based photocatalysis with excellent performance in environment remediation and sustainable energy.

■ ASSOCIATED CONTENT

● Supporting Information

The Supporting Information is available free of charge on the ACS Publications website at DOI: 10.1021/acs.inorgchem.8b01137.

TGA curve (Figures S1), PXRD patterns (Figures S2, S5, and S9), UV-vis spectrum (Figure S3), XPS results (Figures S6–S7), and solid-state PL spectra (Figure S10) (PDF)

Accession Codes

CCDC 1827405 contains the supplementary crystallographic data for this paper. These data can be obtained free of charge via www.ccdc.cam.ac.uk/data_request/cif, or by emailing data_request@ccdc.cam.ac.uk, or by contacting The Cambridge Crystallographic Data Centre, 12 Union Road, Cambridge CB2 1EZ, UK; fax: +44 1223 336033.

■ AUTHOR INFORMATION

Corresponding Authors

*E-mail: chunsenliu@zuzuli.edu.cn.

*E-mail: dumiao@zuzuli.edu.cn.

ORCID

Chun-Sen Liu: 0000-0002-5095-7359

Miao Du: 0000-0002-1029-1820

Notes

The authors declare no competing financial interest.

■ ACKNOWLEDGMENTS

The authors gratefully acknowledge the support from the National Natural Science Foundation of China (Nos. 21601160, 21571158 and 21471134) and the Doctoral Scientific Research Foundation of Zhengzhou University of Light Industry (No.2015BSJJ042).

■ REFERENCES

- (1) Yuan, S.; Qin, J.-S.; Xu, H.-Q.; Su, J.; Rossi, D.; Chen, Y.; Zhang, L.; Lollar, C.; Wang, Q.; Jiang, H.-L.; Son, D. H.; Xu, H.; Huang, Z.; Zou, X.; Zhou, H.-C. [Ti₈Zr₂O₁₂(COO)₁₆] Cluster: An Ideal Inorganic Building Unit for Photoactive Metal–Organic Frameworks. *ACS Cent. Sci.* **2018**, *4*, 105–111.
- (2) Park, J.; Feng, D.; Yuan, S.; Zhou, H.-C. Photochromic Metal–Organic Frameworks: Reversible Control of Singlet Oxygen Generation. *Angew. Chem., Int. Ed.* **2015**, *54*, 430–435.
- (3) Xu, H.-Q.; Hu, J.; Wang, D.; Li, Z.; Zhang, Q.; Luo, Y.; Yu, S.-H.; Jiang, H.-L. Visible-Light Photoreduction of CO₂ in a Metal–Organic Framework: Boosting Electron–Hole Separation via Electron Trap States. *J. Am. Chem. Soc.* **2015**, *137*, 13440–13443.
- (4) Shao, Z.; Huang, C.; Han, X.; Wang, H.; Li, A.; Han, Y.; Li, K.; Hou, H.; Fan, Y. The Effect of Metal Ions on Photocatalytic Performance Based on an Isostructural Framework. *Dalton. Trans.* **2015**, *44*, 12832–12838.
- (5) Liu, L.; Wu, D.; Zhao, B.; Han, X.; Wu, J.; Hou, H.; Fan, Y. Copper(ii) Coordination Polymers: Tunable Structures and a Different Activation Effect of Hydrogen Peroxide for the Degradation of Methyl Orange under Visible Light Irradiation. *Dalton. Trans.* **2015**, *44*, 1406–1411.

- (6) Liu, L.; Ding, J.; Huang, C.; Li, M.; Hou, H.; Fan, Y. Polynuclear Cd II Polymers: Crystal Structures, Topologies, and the Photodegradation for Organic Dye Contaminants. *Cryst. Growth Des.* **2014**, *14*, 3035–3043.

- (7) Costa, M. Toxicity and Carcinogenicity of Cr(VI) in Animal Models and Humans. *Crit. Rev. Toxicol.* **1997**, *27*, 431–442.

- (8) Bhowmik, K.; Mukherjee, A.; Mishra, M. K.; De, G. Stable Ni Nanoparticle–Reduced Graphene Oxide Composites for the Reduction of Highly Toxic Aqueous Cr(VI) at Room Temperature. *Langmuir* **2014**, *30*, 3209–3216.

- (9) Miretzky, P.; Cirelli, A. F. Cr(VI) and Cr(III) Removal from Aqueous Solution by Raw and Modified Lignocellulosic Materials: A Review. *J. Hazard. Mater.* **2010**, *180*, 1–19.

- (10) Rauf, A.; Sher Shah, M. S. A.; Choi, G. H.; Humayoun, U. B.; Yoon, D. H.; Bae, J. W.; Park, J.; Kim, W.-J.; Yoo, P. J. Facile Synthesis of Hierarchically Structured Bi₂S₃/Bi₂WO₆ Photocatalysts for Highly Efficient Reduction of Cr(VI). *ACS Sustainable Chem. Eng.* **2015**, *3*, 2847–2855.

- (11) Liu, X.; Pan, L.; Lv, T.; Zhu, G.; Sun, Z.; Sun, C. Microwave-Assisted Synthesis of CdS–reduced Graphene Oxide Composites for Photocatalytic Reduction of Cr(vi). *Chem. Commun.* **2011**, *47*, 11984–11986.

- (12) Yu, J.; Zhuang, S.; Xu, X.; Zhu, W.; Feng, B.; Hu, J. Photogenerated Electron Reservoir in Hetero-P–n CuO–ZnO Nanocomposite Device for Visible-Light-Driven Photocatalytic Reduction of Aqueous Cr(vi). *J. Mater. Chem. A* **2015**, *3*, 1199–1207.

- (13) Zhang, Y. C.; Li, J.; Zhang, M.; Dionysiou, D. D. Size-Tunable Hydrothermal Synthesis of SnS₂ Nanocrystals with High Performance in Visible Light-Driven Photocatalytic Reduction of Aqueous Cr(VI). *Environ. Sci. Technol.* **2011**, *45*, 9324–9331.

- (14) Lubitz, W.; Tumas, W. Hydrogen: An Overview. *Chem. Rev.* **2007**, *107*, 3900–3903.

- (15) Li, Z.; Xiao, J.-D.; Jiang, H.-L. Encapsulating a Co(II) Molecular Photocatalyst in Metal–Organic Framework for Visible-Light-Driven H₂ Production: Boosting Catalytic Efficiency via Spatial Charge Separation. *ACS Catal.* **2016**, *6*, 5359–5365.

- (16) Qin, J.-S.; Du, D.-Y.; Guan, W.; Bo, X.-J.; Li, Y.-F.; Guo, L.-P.; Su, Z.-M.; Wang, Y.-Y.; Lan, Y.-Q.; Zhou, H.-C. Ultrastable Polymolybdate-Based Metal–Organic Frameworks as Highly Active Electrocatalysts for Hydrogen Generation from Water. *J. Am. Chem. Soc.* **2015**, *137*, 7169–7177.

- (17) Huang, Z.-F.; Song, J.; Li, K.; Tahir, M.; Wang, Y.-T.; Pan, L.; Wang, L.; Zhang, X.; Zou, J.-J. Hollow Cobalt-Based Bimetallic Sulfide Polyhedra for Efficient All-pH-Value Electrochemical and Photocatalytic Hydrogen Evolution. *J. Am. Chem. Soc.* **2016**, *138*, 1359–1365.

- (18) Zhou, H.-C.; Long, J. R.; Yaghi, O. M. Introduction to Metal–Organic Frameworks. *Chem. Rev.* **2012**, *112*, 673–674.

- (19) Zhang, H.; Liu, G.; Shi, L.; Liu, H.; Wang, T.; Ye, J. Engineering Coordination Polymers for Photocatalysis. *Nano Energy* **2016**, *22*, 149–168.

- (20) Wang, H.; Yuan, X.; Wu, Y.; Zeng, G.; Chen, X.; Leng, L.; Wu, Z.; Jiang, L.; Li, H. Facile Synthesis of Amino-Functionalized Titanium Metal–Organic Frameworks and Their Superior Visible-Light Photocatalytic Activity for Cr(VI) Reduction. *J. Hazard. Mater.* **2015**, *286*, 187–194.

- (21) Liang, R.; Shen, L.; Jing, F.; Wu, W.; Qin, N.; Lin, R.; Wu, L. NH₂-Mediated Indium Metal–organic Framework as a Novel Visible-Light-Driven Photocatalyst for Reduction of the Aqueous Cr(VI). *Appl. Catal., B* **2015**, *162*, 245–251.

- (22) Yang, C.; You, X.; Cheng, J.; Zheng, H.; Chen, Y. A Novel Visible-Light-Driven In-Based MOF/graphene Oxide Composite Photocatalyst with Enhanced Photocatalytic Activity toward the Degradation of Amoxicillin. *Appl. Catal., B* **2017**, *200*, 673–680.

- (23) Yan, B.; Zhang, L.; Tang, Z.; Al-Mamun, M.; Zhao, H.; Su, X. Palladium-Decorated Hierarchical Titania Constructed from the Metal–Organic Frameworks NH₂-MIL-125(Ti) as a Robust Photocatalyst for Hydrogen Evolution. *Appl. Catal., B* **2017**, *218*, 743–750.

- (24) Shi, L.; Wang, T.; Zhang, H.; Chang, K.; Meng, X.; Liu, H.; Ye, J. An Amine-Functionalized Iron(III) Metal-Organic Framework as Efficient Visible-Light Photocatalyst for Cr(VI) Reduction. *Adv. Sci.* **2015**, *2*, 1500006.
- (25) Sheldrick, G. M. Crystal Structure Refinement with SHELXL. *Acta Crystallogr., Sect. C: Struct. Chem.* **2015**, *71*, 3–8.
- (26) Spek, A. L. PLATON SQUEEZE: A Tool for the Calculation of the Disordered Solvent Contribution to the Calculated Structure Factors. *Acta Crystallogr., Sect. C: Struct. Chem.* **2015**, *71*, 9–18.
- (27) Zhao, H.; Xia, Q.; Xing, H.; Chen, D.; Wang, H. Construction of Pillared-Layer MOF as Efficient Visible-Light Photocatalysts for Aqueous Cr(VI) Reduction and Dye Degradation. *ACS Sustainable Chem. Eng.* **2017**, *5*, 4449–4456.
- (28) Gong, Y.-N.; Ouyang, T.; He, C.-T.; Lu, T.-B. Photoinduced Water Oxidation by an Organic Ligand Incorporated into the Framework of a Stable Metal-organic Framework. *Chem. Sci.* **2016**, *7*, 1070–1075.
- (29) Liu, Q.; Wu, F.; Cao, F.; Chen, L.; Xie, X.; Wang, W.; Tian, W.; Li, L. A Multijunction of ZnIn₂S₄ nanosheet/TiO₂ film/Si Nanowire for Significant Performance Enhancement of Water Splitting. *Nano Res.* **2015**, *8*, 3524–3534.
- (30) Jing, F.; Liang, R.; Xiong, J.; Chen, R.; Zhang, S.; Li, Y.; Wu, L. MIL-68(Fe) as an Efficient Visible-Light-Driven Photocatalyst for the Treatment of a Simulated Waste-Water Contain Cr(VI) and Malachite Green. *Appl. Catal., B* **2017**, *206*, 9–15.
- (31) Shen, L.; Liang, S.; Wu, W.; Liang, R.; Wu, L. Multifunctional NH₂-Mediated Zirconium Metal-organic Framework as an Efficient Visible-Light-Driven Photocatalyst for Selective Oxidation of Alcohols and Reduction of Aqueous Cr(vi). *Dalton. Trans.* **2013**, *42*, 13649–13657.
- (32) Wang, Q.; Shi, X.; Liu, E.; Crittenden, J. C.; Ma, X.; Zhang, Y.; Cong, Y. Facile Synthesis of AgI/BiOI-Bi₂O₃ Multi-Heterojunctions with High Visible Light Activity for Cr(VI) Reduction. *J. Hazard. Mater.* **2016**, *317*, 8–16.
- (33) Wang, C.-C.; Du, X.-D.; Li, J.; Guo, X.-X.; Wang, P.; Zhang, J. Photocatalytic Cr(VI) Reduction in Metal-Organic Frameworks: A Mini-Review. *Appl. Catal., B* **2016**, *193*, 198–216.
- (34) Padhi, D. K.; Parida, K. Facile Fabrication of α -FeOOH nanorod/RGO Composite: A Robust Photocatalyst for Reduction of Cr(vi) under Visible Light Irradiation. *J. Mater. Chem. A* **2014**, *2*, 10300–10312.
- (35) Liu, P.; Hensen, E. J. M. Highly Efficient and Robust Au/MgCuCr₂O₄ Catalyst for Gas-Phase Oxidation of Ethanol to Acetaldehyde. *J. Am. Chem. Soc.* **2013**, *135*, 14032–14035.
- (36) Xu, Y.; Ye, Y.; Liu, T.; Wang, X.; Zhang, B.; Wang, M.; Han, H.; Li, C. Unraveling a Single-Step Simultaneous Two-Electron Transfer Process from Semiconductor to Molecular Catalyst in a CoPy/CdS Hybrid System for Photocatalytic H₂ Evolution under Strong Alkaline Conditions. *J. Am. Chem. Soc.* **2016**, *138*, 10726–10729.
- (37) Huang, Z.-F.; Song, J.; Li, K.; Tahir, M.; Wang, Y.-T.; Pan, L.; Wang, L.; Zhang, X.; Zou, J.-J. Hollow Cobalt-Based Bimetallic Sulfide Polyhedra for Efficient All-pH-Value Electrochemical and Photocatalytic Hydrogen Evolution. *J. Am. Chem. Soc.* **2016**, *138*, 1359–1365.
- (38) Lee, C.-Y.; Park, H. S.; Fontecilla-Camps, J. C.; Reisner, E. Photoelectrochemical H₂ Evolution with a Hydrogenase Immobilized on a TiO₂-Protected Silicon Electrode. *Angew. Chem., Int. Ed.* **2016**, *55*, 5971–5974.
- (39) Shi, D.; Zheng, R.; Sun, M.-J.; Cao, X.; Sun, C.-X.; Cui, C.-J.; Liu, C.-S.; Zhao, J.; Du, M. Semiconductive Copper(I)-Organic Frameworks for Efficient Light-Driven Hydrogen Generation Without Additional Photosensitizers and Cocatalysts. *Angew. Chem., Int. Ed.* **2017**, *56*, 14637–14641.
- (40) Chen, D.; Xing, H.; Wang, C.; Su, Z. Highly Efficient Visible-Light-Driven CO₂ Reduction to Formate by a New Anthracene-Based Zirconium MOF via Dual Catalytic Routes. *J. Mater. Chem. A* **2016**, *4*, 2657–2662.